

Forecasting sensitivity on tilt of power spectrum of primordial gravitational waves after Planck satellite

This content has been downloaded from IOPscience. Please scroll down to see the full text.

JCAP10(2015)035

(<http://iopscience.iop.org/1475-7516/2015/10/035>)

View [the table of contents for this issue](#), or go to the [journal homepage](#) for more

Download details:

IP Address: 202.141.176.10

This content was downloaded on 15/10/2015 at 10:07

Please note that [terms and conditions apply](#).

Forecasting sensitivity on tilt of power spectrum of primordial gravitational waves after Planck satellite

Qing-Guo Huang,^a Sai Wang^a and Wen Zhao^b

^aState Key Laboratory of Theoretical Physics, Institute of Theoretical Physics, Chinese Academy of Science, Beijing 100190, China

^bCAS Key Laboratory for Researches in Galaxies and Cosmology, Department of Astronomy, University of Science and Technology of China, Chinese Academy of Sciences, Hefei, Anhui 230026, China

E-mail: huangqg@itp.ac.cn, wangsai@itp.ac.cn, wzhao7@ustc.edu.cn

Received September 17, 2015

Accepted September 23, 2015

Published October 13, 2015

Abstract. By taking into account the contamination of foreground radiations, we employ the Fisher matrix to forecast the future sensitivity on the tilt of power spectrum of primordial tensor perturbations for several ground-based (AdvACT, CLASS, Keck/BICEP3, Simons Array, SPT-3G), balloon-borne (EBEX, Spider) and satellite (CMBPol, COrE, LiteBIRD) experiments of B-mode polarizations. For the fiducial model $n_t = 0$, our results show that the satellite experiments give good sensitivity on the tensor tilt n_t to the level $\sigma_{n_t} \lesssim 0.1$ for $r \gtrsim 2 \times 10^{-3}$, while the ground-based and balloon-borne experiments give worse sensitivity. By considering the BICEP2/Keck Array and Planck (BKP) constraint on the tensor-to-scalar ratio r , we see that it is impossible for these experiments to test the consistency relation $n_t = -r/8$ in the canonical single-field slow-roll inflation models.

Keywords: CMBR polarisation, gravitational waves and CMBR polarization

ArXiv ePrint: [1509.02676](https://arxiv.org/abs/1509.02676)

Contents

1	Introduction	1
2	Signal, foregrounds and noise	2
3	Likelihood and Fisher matrix	4
4	Analysis and results	5
5	Discussion	5
A	Instrumental specifications	9

1 Introduction

The inflation paradigm [1–5] predicts the primordial gravitational waves, i.e. tensor perturbations. The primordial gravitational waves can contribute to the total intensity and polarizations of cosmic microwave background (CMB) anisotropy [6–12]. From the recent Planck TT,TE,EE+lowP data release [13], the upper limit on tensor-to-scalar ratio is given by $r_{0.002} < 0.11$ at the 95% confidence level (C.L.) by fitting the Λ CDM+r model. The B-mode polarizations contributed by primordial gravitational waves may be detectable at the range $\ell \lesssim 150$. Actually, BICEP2 [14] has pushed the sensitivity of B-mode polarizations to be comparable with that of temperature in searching for the primordial gravitational waves. However, the polarized dust emissions make us difficult to distinguish whether the detected B-mode power comes from the primordial gravitational waves [15–18]. Recently, Planck [19] released the full-sky data of polarized dust emissions. Based on this, a joint analysis of the B-mode data from BICEP2/Keck Array and Planck (BKP) [20] yielded an upper bound $r_{0.05} < 0.12$ at the 95% C.L., which is compatible with the upper limit from Planck data without the B-mode polarizations.

The tilt of power spectrum of primordial tensor perturbations is used to measure the feature of the primordial gravitational waves. In the power spectrum of primordial tensor perturbations, the tensor tilt n_t is defined by

$$P_t(k) = r A_s \left(\frac{k}{k_p} \right)^{n_t}, \quad (1.1)$$

where $P_t(k)$ is the amplitude of power spectrum of primordial tensor perturbations at the scale k , r denotes the tensor-to-scalar ratio at a given pivot scale k_p and A_s the amplitude of primordial scalar perturbations which is set as a constant in this paper. In the inflation model, the tensor tilt is generally predicted as $n_t = -2\epsilon$ [21, 22]. The inflation requires $\ddot{a}/a = H^2(1 - \epsilon)$ where $\epsilon = \dot{H}/H^2$, and thus $-2 < n_t < 0$. In the canonical single-field slow-roll inflation models, the tensor tilt is determined by the tensor-to-scalar ratio via the consistency relation, i.e. $n_t = -r/8$ [21]. By considering the upper bounds on r , we expect the power spectrum of primordial gravitational waves to be nearly scale-invariant, i.e. $n_t \simeq 0$. The current constraint on n_t was given by $n_{t,0.01} = -0.76^{+1.37}_{-0.52}$ [23] at the 68% C.L. by combining only the BKP B-mode data and the upper limit on the intensity of stochastic

gravitational wave background from Laser Interferometer Gravitational-Waves Observatory (LIGO) [24]. The scale-invariant spectrum is well compatible with this constraint.

Even though at present there are no evidence for the primordial gravitational waves, several future polarization experiments might reach the sensitivity to detect the primordial gravitational waves in the coming years. As a recent analysis, ref. [25] forecasted that the primordial gravitational waves with theoretically motivated $r \sim 2 \times 10^{-3}$ can be achievable by certain future experiments if the noise is reduced to $\sim 1 \mu K$ -arcmin and the lensing B-modes reduced to 10%. Their forecasts are not changed significantly with respect to previous estimates [26]. In this paper, we study the sensitivity on the tensor tilt n_t for several future ground-based (AdvACT, CLASS, Keck/BICEP3, Simons Array, SPT-3G), balloon-borne (EBEX, Spider) and satellite (CMBPol, COrE, LiteBIRD) experiments. We are just interested in studying the nearly scale-invariant case, i.e. $n_t \simeq 0$ which corresponds to a class of the simplest inflation models. Similar to ref. [25], the approach of Fisher matrix is also used in our analysis. The paper is arranged as follows. The B-mode polarizations, foregrounds and noise sources are described in section 2. In section 3, the method used in this paper is revealed. In section 4, we show our forecasts for the future experiments. Conclusions and discussion are given in section 5.

2 Signal, foregrounds and noise

In general, the CMB linear polarizations can be expressed in terms of the spin-weighted spherical harmonics $_{\pm 2}Y_{\ell m}$, namely

$$Q \pm iU = \sum_{\ell m} a_{\ell m}^{\pm 2} {}_{\pm 2}Y_{\ell m}, \quad (2.1)$$

or equivalently, defined by the E- and B-modes as

$$E = \sum_{\ell m} a_{\ell m}^E Y_{\ell m}, \quad (2.2)$$

$$B = \sum_{\ell m} a_{\ell m}^B Y_{\ell m}, \quad (2.3)$$

where the coefficients are given by

$$a_{\ell m}^E = -\frac{1}{2} (a_{\ell m}^{+2} + a_{\ell m}^{-2}), \quad (2.4)$$

$$a_{\ell m}^B = -\frac{1}{2i} (a_{\ell m}^{+2} - a_{\ell m}^{-2}). \quad (2.5)$$

In this paper, we are just focused on studying the B-modes which may include the signal of primordial gravitational waves.

In the linear perturbation theory, the primordial B-modes are Gaussian with zero mean, and their variance is given by

$$\langle a_{\ell m}^B a_{\ell' m'}^{B*} \rangle = C_{\ell}^{BB} \delta_{\ell \ell'} \delta_{m m'}, \quad (2.6)$$

where δ comes from statistical isotropy. As conventions, the angular correlation coefficients between B-modes are defined as

$$\tilde{C}_{\ell} = \frac{\ell(\ell+1)}{2\pi} C_{\ell}^{BB}, \quad (2.7)$$

Parameters	Synchrotron	Thermal Dust
$A_{72\%}$	2.1×10^{-5}	0.169
$A_{53\%}$	2.1×10^{-5}	0.065
$A_{24\%}$	2.1×10^{-5}	0.019
$A_{11\%}$	4.2×10^{-6}	0.013
$A_{1\%}$	4.2×10^{-6}	0.006
$\nu[GHz]$	65	353
ℓ	80	80
α	-2.6	-2.42
β	-2.9	1.59
$T[K]$	—	19.6

Table 1. A list of foreground parameters [16, 19, 25, 30]. Here $A_{f_{sky}}$ denotes the cleanest effective area f_{sky} in the sky and its unit is μK^2 .

where we have dropped the superscript BB for simplicity. In our study, we generate the power spectrum of primordial B-modes by running the CAMB package [27, 28], and we set all the cosmological parameters except r and n_t to the best-fit values of Planck 2015 results [29]. However, we should find out a reasonable pivot scale k_p such that there is least degeneracy between r and n_t in eq. (1.1).

The foregrounds contaminate the CMB B-mode signal and should be taken into account in the forecast. Actually, we can separate each component of foregrounds by noting that they have very different frequency-dependence. The Galactic synchrotron emission (S) and thermal dust emission (D) are considered in this paper. Their power spectra are given by

$$S_{\ell\nu} = (W_\nu^S)^2 C_\ell^S = (W_\nu^S)^2 A_S \left(\frac{\ell}{\ell_S} \right)^{\alpha_S}, \quad (2.8)$$

$$D_{\ell\nu} = (W_\nu^D)^2 C_\ell^D = (W_\nu^D)^2 A_D \left(\frac{\ell}{\ell_D} \right)^{\alpha_D}, \quad (2.9)$$

where various parameters can be found in table 1, and W_ν^S and W_ν^D are defined by

$$W_\nu^S = \frac{W_{\nu_S}^{CMB}}{W_\nu^{CMB}} \left(\frac{\nu}{\nu_S} \right)^{\beta_S}, \quad (2.10)$$

$$W_\nu^D = \frac{W_{\nu_D}^{CMB}}{W_\nu^{CMB}} \left(\frac{\nu}{\nu_D} \right)^{1+\beta_D} \frac{e^{h\nu_D/k_B T} - 1}{e^{h\nu/k_B T} - 1}, \quad (2.11)$$

$$W_\nu^{CMB} = \frac{x^2 e^x}{(e^x - 1)^2}, \quad x = \frac{h\nu}{k_B T_{CMB}}. \quad (2.12)$$

Here we have rescaled the temperature of Galactic synchrotron emission and thermal dust emission with respect to the CMB temperature. There might be certain correlation between

synchrotron emission and dust emission. To account for this, we assume their correlation taking the form $g\sqrt{S_{\ell\nu_i}D_{\ell\nu_j}}$ in the power spectra.

In this paper, we do not consider the systematics which strongly depend on the experimental setups. However, we consider the instrumental white noise which is Gaussian. The power spectrum of the white noise can be expressed as [31]

$$\mathcal{N}_\ell = \frac{\ell(\ell+1)}{2\pi} \delta P^2 e^{\ell^2 \sigma_b^2}, \quad (2.13)$$

where δP denotes the sensitivity for the Stokes parameters Q and U, and $\sigma_b = 0.425\theta_{FWHM}$ denotes the beam-size variance. Various instrumental parameters here can be found in table 5 in appendix.

The gravitational lensing can also limit our ability to detect primordial B-mode polarizations. However, the lensing B-modes and primordial B-modes have the same frequency-dependence, and we cannot separate them as mentioned above. Fortunately, one can reconstruct the lensing potential by considering the CMB data of temperature and E-mode polarizations at small angular scales, and then remove the lensing B-modes away at large angular scales [42–45]. In this paper, we assume the power of lensing B-modes reduced to 10% of its original value for the CMBPol and COrE experiments. For others, it is marginal to employ delensing [25]. The residual power $\delta C_\ell^{\text{delensing}}$ of lensing B-modes can be incorporated into the power spectrum of an effective noise, i.e. $\mathcal{N}_\ell \rightarrow \mathcal{N}_\ell + \delta C_\ell^{\text{delensing}}$ [26].

3 Likelihood and Fisher matrix

As mentioned above, we will deal with three components of CMB B-modes which originate from primordial gravitational waves, Galactic dust and synchrotron emissions, respectively. In the “Component Separation” (CS) method, the average of log-likelihood can be given by [25]

$$\langle \log \mathcal{L}_{BB} \rangle = -\frac{1}{2} \sum_\ell (2\ell+1) f_{sky} \left(\log \det \left(\frac{W\bar{C}_\ell W^T + \mathcal{N}_\ell}{\bar{W}\bar{C}_\ell \bar{W}^T + \mathcal{N}_\ell} \right) + \text{tr} \left(\frac{\bar{W}\bar{C}_\ell \bar{W}^T + \mathcal{N}_\ell}{W\bar{C}_\ell W^T + \mathcal{N}_\ell} - 1 \right) \right), \quad (3.1)$$

where the bar denotes all the parameters fixed to their “true” values, and we have used the normalization such that $\langle \log \mathcal{L}_{BB} \rangle = 0$ for $\bar{C}_\ell = C_\ell$ and $\bar{W} = W$. Here W denotes the frequency-dependence of each component of CMB B-modes, which is a $3 \times N$ matrix with a row $(1, W_{\nu_i}^D, W_{\nu_i}^S)$. N denotes the number of frequency channels for each experiment. C_ℓ is the covariance matrix of the amplitudes of three components. f_{sky} stands for the effective area of the sky in table 5, where each experiment observes.

In our consideration, the average of log-likelihood is a function of several parameters \mathbf{p} which are $(r, n_t, A_D, A_S, \beta_D, \beta_S, g)$. We assume Gaussian priors for A_D , A_S , β_D and β_S with the variance of 50%, 50%, 15% and 10%. Based on eq. (3.1), the Fisher matrix is defined by

$$F_{ij} = - \frac{\partial^2 \langle \log \mathcal{L}_{BB} \rangle}{\partial p_i \partial p_j} \Big|_{\mathbf{p}=\bar{\mathbf{p}}}, \quad (3.2)$$

where $\bar{\mathbf{p}}$ denote “true” values of the parameters \mathbf{p} . In our fiducial model, we set $\bar{g} = 0.5$ and $\bar{n}_t = 0$. The minimum error on the parameter p_i is given by the Cramer-Rao bound, i.e.

$$\sigma_{p_i}^2 \geq (F^{-1})_{ii}. \quad (3.3)$$

In this paper, we will forecast the future sensitivity on both r and n_t simultaneously, since primordial gravitational waves are not detected until now. There could be certain correlation between r and n_t , or equivalently, the (r, n_t) confidence ellipse has a tilt. Thus we should find a pivot scale k_p to make their correlation to be least. In other words, we should find the pivot scale such that $(F^{-1})_{rn_t} = 0$, which minimizes the constraint on r .

4 Analysis and results

For the future ground-based experiments, we consider the CMB multipoles of the range $[30, 150]$ for Keck/BICEP3, Simons Array and SPT-3G, while $[2, 150]$ for AdvACT and CLASS. The reason is that AdvACT and CLASS cover a larger fraction of the sky. We forecast on the future sensitivity on r and n_t by using the Fisher matrix. The 1σ errors on r and n_t can be found in table 2. We also list the pivot scale $k_p[\text{Mpc}^{-1}]$ at which there is no tilt for the (r, n_t) confidence ellipse. We found that the ground-based experiments can probe the tensor-to-scalar ratio to the level $r \simeq 0.01$, which is consistent with previous estimates. The 1σ error on the tensor tilt is to the level $\sigma_{n_t} \sim 0.1$ when $2 \times 10^{-3} < r < 0.1$ for AdvACT and CLASS, while $\sigma_{n_t} \gtrsim 1$ for other three experiments.

For the future balloon-borne experiments, we consider the CMB multipoles of the range $[30, 150]$. The 1σ errors on r and n_t and the pivot scale k_p can be found in table 3. We find that EBEX and Spider can marginally probe the tensor-to-scalar ratio to the level $r \simeq 0.02$, which is consistent with previous estimates. The 1σ error on the tensor tilt is $\sigma_{n_t} > 1$ when $2 \times 10^{-3} < r < 0.1$.

For the future satellite experiments, we consider the CMB multipoles of the range $[2, 300]$ for CMBPol and CORe while $[2, 150]$ for LiteBIRD. The 1σ errors on r and n_t and the pivot scale k_p can be found in table 4. The delensing has been taken into account for CMBPol and CORe. We find that the satellite experiments can well probe the tensor-to-scalar ratio even to the level $r \simeq 2 \times 10^{-3}$, which is also consistent with previous estimates. The 1σ error on the tensor tilt n_t runs from ~ 0.1 to ~ 0.01 when r runs from 2×10^{-3} to 0.1 . Thus the future satellite experiments provide the highest sensitivity on the tensor tilt n_t by contrast to the future ground-based and balloon-borne experiments.

We plot the (r, n_t) confidence ellipses of 1σ and 2σ C.L. for the CLASS and LiteBIRD experiments in figure 1. Here the fiducial parameters are chosen as $r = 0.01$ and $n_t = 0$. AdvACT and CLASS denote the best sensitivity on both r and n_t in the five future ground-based experiments. Unfortunately, they can not still compare with the future satellite experiments such as LiteBIRD. Even though the satellite experiments give the best sensitivity on n_t , it is impossible for them to test the consistent relation, i.e. $n_t = -r/8$. By considering the BKP constraint $r_{0.05} < 0.12$ at 95% C.L., we deduce $n_t < 0.015$ which is much smaller than the 1σ errors on n_t in table 4.

5 Discussion

In this paper, we forecasted the sensitivity on the tensor tilt n_t for future ground-based, balloon-borne and satellite experiments of B-mode polarizations. We focused on the scale-invariant power spectrum $n_t = 0$ which approximately corresponds to the canonical single-field slow-roll inflation models. For the tensor tilt, the satellite experiments can give a good sensitivity on n_t even for $r \simeq 2 \times 10^{-3}$. Specifically, the 1σ error on n_t varies from ~ 0.1

	r	σ_r	σ_{n_t}	$k_p[\text{Mpc}^{-1}]$
AdvACT	0.1	5.3×10^{-3}	9.7×10^{-2}	8.4×10^{-3}
	0.05	4.4×10^{-3}	1.2×10^{-1}	7.5×10^{-3}
	0.02	3.6×10^{-3}	1.6×10^{-1}	5.2×10^{-3}
	0.01	3.1×10^{-3}	2.3×10^{-1}	3.4×10^{-3}
	0.005	2.6×10^{-3}	3.6×10^{-1}	2.1×10^{-3}
	0.002	2.1×10^{-3}	7.5×10^{-1}	1.3×10^{-3}
CLASS	0.1	6.7×10^{-3}	9.0×10^{-2}	6.3×10^{-3}
	0.05	5.5×10^{-3}	1.1×10^{-1}	4.7×10^{-3}
	0.02	4.1×10^{-3}	1.6×10^{-1}	2.4×10^{-3}
	0.01	3.1×10^{-3}	2.5×10^{-1}	1.3×10^{-3}
	0.005	2.2×10^{-3}	4.2×10^{-1}	8.6×10^{-4}
	0.002	1.5×10^{-3}	9.3×10^{-1}	5.7×10^{-4}
Keck/BICEP3	0.1	2.3×10^{-2}	1.2	9.2×10^{-3}
	0.05	1.7×10^{-2}	1.8	8.9×10^{-3}
	0.02	1.4×10^{-2}	3.6	8.7×10^{-3}
	0.01	1.3×10^{-2}	6.6	8.7×10^{-3}
	0.005	1.2×10^{-2}	12.5	8.6×10^{-3}
	0.002	1.2×10^{-2}	30.4	8.6×10^{-3}
Simons Array	0.1	1.7×10^{-2}	7.0×10^{-1}	9.3×10^{-3}
	0.05	1.5×10^{-2}	1.3	9.3×10^{-3}
	0.02	1.4×10^{-2}	3.0	9.2×10^{-3}
	0.01	1.4×10^{-2}	5.9	9.2×10^{-3}
	0.005	1.4×10^{-2}	11.7	9.2×10^{-3}
	0.002	1.4×10^{-2}	29.1	9.2×10^{-3}
SPT-3G	0.1	8.8×10^{-3}	4.3×10^{-1}	9.4×10^{-3}
	0.05	6.6×10^{-3}	6.4×10^{-1}	9.2×10^{-3}
	0.02	5.3×10^{-3}	1.3	9.1×10^{-3}
	0.01	4.8×10^{-3}	2.3	9.1×10^{-3}
	0.005	4.5×10^{-3}	4.4	9.0×10^{-3}
	0.002	4.4×10^{-3}	10.6	9.0×10^{-3}

Table 2. 1σ errors on r and n_t for future ground-based experiments. The pivot scale $k_p[\text{Mpc}^{-1}]$ is also listed, at which there is no correlation between r and n_t and then the (r, n_t) confidence ellipse has no tilt.

	r	σ_r	σ_{n_t}	$k_p[\text{Mpc}^{-1}]$
EBEX	0.1	2.3×10^{-2}	1.2	9.1×10^{-3}
	0.05	1.7×10^{-2}	1.9	8.8×10^{-3}
	0.02	1.3×10^{-2}	3.7	8.6×10^{-3}
	0.01	1.2×10^{-2}	6.8	8.4×10^{-3}
	0.005	1.1×10^{-2}	12.9	8.4×10^{-3}
	0.002	1.0×10^{-2}	31.4	8.4×10^{-3}
Spider	0.1	1.8×10^{-2}	1.0	8.6×10^{-3}
	0.05	1.5×10^{-2}	1.8	8.4×10^{-3}
	0.02	1.4×10^{-2}	4.1	8.3×10^{-3}
	0.01	1.3×10^{-2}	7.9	8.3×10^{-3}
	0.005	1.3×10^{-2}	15.4	8.3×10^{-3}
	0.002	1.3×10^{-2}	38.2	8.3×10^{-3}

Table 3. 1σ errors on r and n_t for future balloon-borne experiments. The pivot scale $k_p[\text{Mpc}^{-1}]$ is also listed correspondingly.

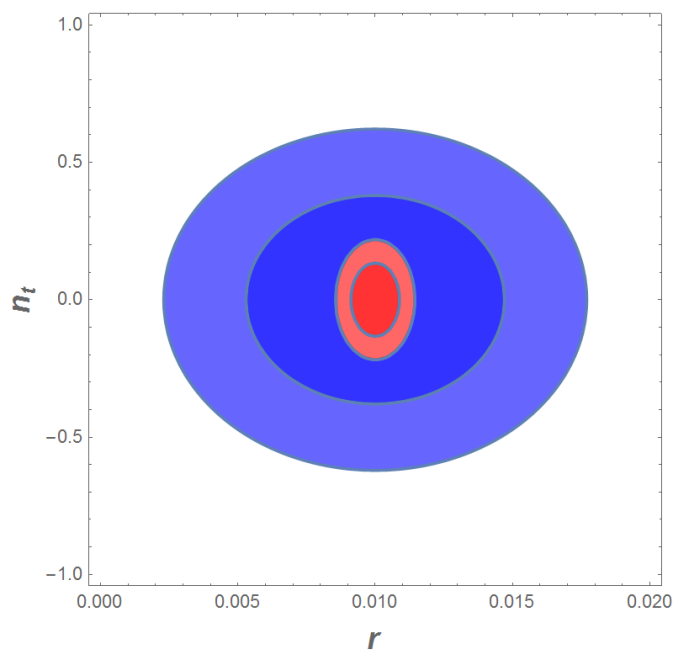


Figure 1. The (r, n_t) confidence ellipses of 1σ and 2σ C.L. for CLASS (blue) and LiteBIRD (red). The fiducial parameters are given by $r = 0.01$ and $n_t = 0$.

	r	σ_r	σ_{n_t}	$k_p[\text{Mpc}^{-1}]$
CMBPol	0.1	1.2×10^{-3}	3.0×10^{-2}	1.1×10^{-2}
	0.05	7.1×10^{-4}	3.8×10^{-2}	1.0×10^{-2}
	0.02	3.8×10^{-4}	5.1×10^{-2}	9.0×10^{-3}
	0.01	2.5×10^{-4}	6.2×10^{-2}	8.4×10^{-3}
	0.005	1.8×10^{-4}	7.5×10^{-2}	7.9×10^{-3}
	0.002	1.4×10^{-4}	9.7×10^{-2}	7.2×10^{-3}
COrE	0.1	1.3×10^{-3}	3.4×10^{-2}	1.1×10^{-2}
	0.05	8.2×10^{-4}	4.4×10^{-2}	9.7×10^{-3}
	0.02	4.6×10^{-4}	5.8×10^{-2}	8.6×10^{-3}
	0.01	3.3×10^{-4}	7.0×10^{-2}	8.1×10^{-3}
	0.005	2.5×10^{-4}	8.3×10^{-2}	7.5×10^{-3}
	0.002	2.1×10^{-4}	1.1×10^{-1}	6.3×10^{-3}
LiteBIRD	0.1	1.8×10^{-3}	5.3×10^{-2}	8.9×10^{-3}
	0.05	1.1×10^{-3}	6.1×10^{-2}	8.5×10^{-3}
	0.02	7.3×10^{-4}	7.5×10^{-2}	8.0×10^{-3}
	0.01	5.8×10^{-4}	8.8×10^{-2}	7.1×10^{-3}
	0.005	4.9×10^{-4}	1.1×10^{-1}	6.2×10^{-3}
	0.002	4.4×10^{-4}	1.7×10^{-1}	5.3×10^{-3}

Table 4. 1σ errors on r and n_t for future satellite experiments. The pivot scale $k_p[\text{Mpc}^{-1}]$ is also listed correspondingly.

to ~ 0.01 when r varies from ~ 0.001 to ~ 0.1 . By contrast, the ground-based and balloon-borne experiments give much worse sensitivity on both r and n_t . Furthermore, our results did not change significantly with respect to previous forecasts on the future sensitivity of tensor-to-scalar ratio r in ref. [25]. The reason is that we just considered the scale-invariant tensor tilt $n_t = 0$ in our fiducial model. By considering the BKP constraint on r , we see that it is impossible for these future experiments to test the consistent relation $n_t = -r/8$ in the canonical single-field slow-roll inflation models.

Acknowledgments

Q.G.H. and S.W. are supported by grants from NSFC (grant NO. 11322545, 11335012 and 11575271). W.Z. is supported by Project 973 under Grant No. 2012CB821804, by NSFC No. 11173021, 11322324, 11421303 and project of KIP and CAS.

A Instrumental specifications

Experiments	$f_{\text{sky}}[\%]$	$\nu[\text{GHz}]$	$\theta_{FWHM}[']$	$\delta P[\mu K']$
AdvACT	50	90	2.2	7.8
	50	150	1.3	6.9
	50	230	0.9	25
CLASS	70	38	90	39
	70	93	40	13
	70	148	24	15
	70	217	18	43
Keck/BICEP3	1	95	30	9.0
	1	150	30	2.3
	1	220	30	10
Simons Array	20	90	5.2	15.2
	20	150	3.5	12.3
	20	220	2.7	23.6
SPT-3G	6	95	1	6.0
	6	150	1	3.5
	6	220	1	6.0
EBEX	1	150	8	5.8
	1	250	8	17
	1	410	8	150
Spider	7.5	94	49	17.8
	7.5	150	30	13.6
	7.5	280	17	52.6
CMBPol	70	30	26	19.2
	70	45	17	8.3
	70	70	11	4.2
	70	100	8	3.2
	70	150	5	3.1
	70	220	3.5	4.8
	70	340	2.3	21.6
COrE	70	45	23	9.1
	70	75	14	4.7
	70	105	10	4.6
	70	135	7.8	4.6
	70	165	6.4	4.6
	70	195	5.4	4.5
	70	225	4.7	4.6
	70	255	4.1	10.5
	70	285	3.7	17.4
	70	315	3.3	46.6
	70	375	2.8	119
LiteBIRD	70	60	32	10.3
	70	78	58	6.5
	70	100	45	4.7
	70	140	32	3.7
	70	195	24	3.1
	70	280	16	3.8

Table 5. Instrumental specifications of future ground-based, balloon-borne and satellite experiments [32–41]. Here $\delta P = \sigma_{\text{pix}} \theta_{FWHM}$.

References

- [1] A.A. Starobinsky, *Spectrum of relict gravitational radiation and the early state of the universe*, *JETP Lett.* **30** (1979) 682 [[INSPIRE](#)].
- [2] A.A. Starobinsky, *A new type of isotropic cosmological models without singularity*, *Phys. Lett. B* **91** (1980) 99 [[INSPIRE](#)].
- [3] A.H. Guth, *The inflationary universe: a possible solution to the horizon and flatness problems*, *Phys. Rev. D* **23** (1981) 347 [[INSPIRE](#)].
- [4] A.D. Linde, *A new inflationary universe scenario: a possible solution of the horizon, flatness, homogeneity, isotropy and primordial monopole problems*, *Phys. Lett. B* **108** (1982) 389 [[INSPIRE](#)].
- [5] A. Albrecht and P.J. Steinhardt, *Cosmology for grand unified theories with radiatively induced symmetry breaking*, *Phys. Rev. Lett.* **48** (1982) 1220 [[INSPIRE](#)].
- [6] L.P. Grishchuk, *Amplification of gravitational waves in an isotropic universe*, *Sov. Phys. JETP* **40** (1975) 409 [*Zh. Eksp. Teor. Fiz.* **67** (1974) 825] [[INSPIRE](#)].
- [7] A.A. Starobinsky, *Spectrum of relict gravitational radiation and the early state of the universe*, *JETP Lett.* **30** (1979) 682 [*Pisma Zh. Eksp. Teor. Fiz.* **30** (1979) 719] [[INSPIRE](#)].
- [8] V.A. Rubakov, M.V. Sazhin and A.V. Veryaskin, *Graviton creation in the inflationary universe and the grand unification scale*, *Phys. Lett. B* **115** (1982) 189 [[INSPIRE](#)].
- [9] R. Crittenden, J.R. Bond, R.L. Davis, G. Efstathiou and P.J. Steinhardt, *The imprint of gravitational waves on the cosmic microwave background*, *Phys. Rev. Lett.* **71** (1993) 324 [[astro-ph/9303014](#)] [[INSPIRE](#)].
- [10] M. Kamionkowski, A. Kosowsky and A. Stebbins, *A probe of primordial gravity waves and vorticity*, *Phys. Rev. Lett.* **78** (1997) 2058 [[astro-ph/9609132](#)] [[INSPIRE](#)].
- [11] M. Kamionkowski, A. Kosowsky and A. Stebbins, *Statistics of cosmic microwave background polarization*, *Phys. Rev. D* **55** (1997) 7368 [[astro-ph/9611125](#)] [[INSPIRE](#)].
- [12] W. Hu, U. Seljak, M.J. White and M. Zaldarriaga, *A complete treatment of CMB anisotropies in a FRW universe*, *Phys. Rev. D* **57** (1998) 3290 [[astro-ph/9709066](#)] [[INSPIRE](#)].
- [13] PLANCK collaboration, P.A.R. Ade et al., *Planck 2015 results. XX. Constraints on inflation*, [arXiv:1502.02114](#) [[INSPIRE](#)].
- [14] BICEP2 collaboration, P.A.R. Ade et al., *Detection of B-mode polarization at degree angular scales by BICEP2*, *Phys. Rev. Lett.* **112** (2014) 241101 [[arXiv:1403.3985](#)] [[INSPIRE](#)].
- [15] M.J. Mortonson and U. Seljak, *A joint analysis of Planck and BICEP2 B modes including dust polarization uncertainty*, *JCAP* **10** (2014) 035 [[arXiv:1405.5857](#)] [[INSPIRE](#)].
- [16] R. Flauger, J.C. Hill and D.N. Spergel, *Toward an understanding of foreground emission in the BICEP2 region*, *JCAP* **08** (2014) 039 [[arXiv:1405.7351](#)] [[INSPIRE](#)].
- [17] W.N. Colley and J.R. Gott, *Genus topology and cross-correlation of BICEP2 and Planck 353 GHz B-modes: further evidence favouring gravity wave detection*, *Mon. Not. Roy. Astron. Soc.* **447** (2015) 2034 [[arXiv:1409.4491](#)] [[INSPIRE](#)].
- [18] C. Cheng, Q.-G. Huang and S. Wang, *Constraint on the primordial gravitational waves from the joint analysis of BICEP2 and Planck HFI 353 GHz dust polarization data*, *JCAP* **12** (2014) 044 [[arXiv:1409.7025](#)] [[INSPIRE](#)].
- [19] PLANCK collaboration, R. Adam et al., *Planck intermediate results. XXX. The angular power spectrum of polarized dust emission at intermediate and high Galactic latitudes*, [arXiv:1409.5738](#) [[INSPIRE](#)].

- [20] BICEP2, PLANCK collaboration, P. Ade et al., *Joint analysis of BICEP2/Keck Array and Planck data*, *Phys. Rev. Lett.* **114** (2015) 101301 [[arXiv:1502.00612](#)] [[INSPIRE](#)].
- [21] A.R. Liddle and D.H. Lyth, *COBE, gravitational waves, inflation and extended inflation*, *Phys. Lett. B* **291** (1992) 391 [[astro-ph/9208007](#)] [[INSPIRE](#)].
- [22] J. Garriga and V.F. Mukhanov, *Perturbations in k-inflation*, *Phys. Lett. B* **458** (1999) 219 [[hep-th/9904176](#)] [[INSPIRE](#)].
- [23] Q.-G. Huang and S. Wang, *No evidence for the blue-tilted power spectrum of relic gravitational waves*, *JCAP* **06** (2015) 021 [[arXiv:1502.02541](#)] [[INSPIRE](#)].
- [24] VIRGO, LIGO SCIENTIFIC collaboration, J. Aasi et al., *Improved upper limits on the stochastic gravitational-wave background from 2009–2010 LIGO and Virgo Data*, *Phys. Rev. Lett.* **113** (2014) 231101 [[arXiv:1406.4556](#)] [[INSPIRE](#)].
- [25] P. Creminelli, D.L. Nacir, M. Simonovic, G. Trevisan and M. Zaldarriaga, *Detecting primordial B-modes after Planck*, [arXiv:1502.01983](#) [[INSPIRE](#)].
- [26] H. Lee, S.C. Su and D. Baumann, *The superhorizon test of future B-mode experiments*, *JCAP* **02** (2015) 036 [[arXiv:1408.6709](#)] [[INSPIRE](#)].
- [27] A. Lewis, A. Challinor and A. Lasenby, *Efficient computation of CMB anisotropies in closed FRW models*, *Astrophys. J.* **538** (2000) 473 [[astro-ph/9911177](#)] [[INSPIRE](#)].
- [28] C. Howlett, A. Lewis, A. Hall and A. Challinor, *CMB power spectrum parameter degeneracies in the era of precision cosmology*, *JCAP* **04** (2012) 027 [[arXiv:1201.3654](#)] [[INSPIRE](#)].
- [29] PLANCK collaboration, P.A.R. Ade et al., *Planck 2015 results. XIII. Cosmological parameters*, [arXiv:1502.01589](#) [[INSPIRE](#)].
- [30] WMAP collaboration, L. Page et al., *Three year Wilkinson Microwave Anisotropy Probe (WMAP) observations: polarization analysis*, *Astrophys. J. Suppl.* **170** (2007) 335 [[astro-ph/0603450](#)] [[INSPIRE](#)].
- [31] L. Knox, *Determination of inflationary observables by cosmic microwave background anisotropy experiments*, *Phys. Rev. D* **52** (1995) 4307 [[astro-ph/9504054](#)] [[INSPIRE](#)].
- [32] E. Calabrese et al., *Precision epoch of reionization studies with next-generation CMB experiments*, *JCAP* **08** (2014) 010 [[arXiv:1406.4794](#)] [[INSPIRE](#)].
- [33] B. Reichborn-Kjennerud, *Building and flying the E and B Experiment to measure the polarization of the cosmic microwave background*, Ph.D. thesis, Columbia University, New York U.S.A. (2010).
- [34] R.W. Ogburn, IV et al., *BICEP2 and Keck Array operational overview and status of observations*, *Proc. SPIE Int. Soc. Opt. Eng.* **8452** (2012) 1A [[arXiv:1208.0638](#)] [[INSPIRE](#)].
- [35] A. Lee, *The POLARBEAR-1, POLARBEAR-2, and Simons Array Experiments*, http://max.ifca.unican.es/EPI2013/epi2013_talks/Thursday/EPI_27062013_01_Lee.pdf (2013).
- [36] SPT-3G collaboration, B.A. Benson et al., *SPT-3G: a next-generation Cosmic Microwave background polarization experiment on the South Pole Telescope*, *Proc. SPIE Int. Soc. Opt. Eng.* **9153** (2014) 91531P [[arXiv:1407.2973](#)] [[INSPIRE](#)].
- [37] A.A. Fraisse et al., *SPIDER: probing the early universe with a suborbital polarimeter*, *JCAP* **04** (2013) 047 [[arXiv:1106.3087](#)] [[INSPIRE](#)].
- [38] A.S. Rahlin et al., *Pre-flight integration and characterization of the SPIDER balloon-borne telescope*, *Proc. SPIE Int. Soc. Opt. Eng.* **9153** (2014) 915313 [[arXiv:1407.2906](#)] [[INSPIRE](#)].
- [39] CMBPOL STUDY TEAM collaboration, D. Baumann et al., *CMBPol mission concept study: probing inflation with CMB polarization*, *AIP Conf. Proc.* **1141** (2009) 10 [[arXiv:0811.3919](#)] [[INSPIRE](#)].

- [40] CORE collaboration, F.R. Bouchet et al., *COrE (Cosmic Origins Explorer) a white paper*, [arXiv:1102.2181](#) [INSPIRE].
- [41] T. Matsumura et al., *Mission design of LiteBIRD*, [arXiv:1311.2847](#) [INSPIRE].
- [42] L. Knox and Y.-S. Song, *A limit on the detectability of the energy scale of inflation*, *Phys. Rev. Lett.* **89** (2002) 011303 [[astro-ph/0202286](#)] [INSPIRE].
- [43] M. Kesden, A. Cooray and M. Kamionkowski, *Separation of gravitational wave and cosmic shear contributions to cosmic microwave background polarization*, *Phys. Rev. Lett.* **89** (2002) 011304 [[astro-ph/0202434](#)] [INSPIRE].
- [44] U. Seljak and C.M. Hirata, *Gravitational lensing as a contaminant of the gravity wave signal in CMB*, *Phys. Rev. D* **69** (2004) 043005 [[astro-ph/0310163](#)] [INSPIRE].
- [45] K.M. Smith, D. Hanson, M. LoVerde, C.M. Hirata and O. Zahn, *Delensing CMB polarization with external datasets*, *JCAP* **06** (2012) 014 [[arXiv:1010.0048](#)] [INSPIRE].